Biophysical Journal
Article

Biophysical Society

Phase transitions of the pulmonary surfactant film at the perfluorocarbon-water interface

Guangle Li,[1] Xiaojie Xu,[1] and Yi Y. Zuo[1,2,*]
[1]Department of Mechanical Engineering, University of Hawaii at Manoa, Honolulu, Hawaii and [2]Department of Pediatrics, John A. Burns School of Medicine, University of Hawaii, Honolulu, Hawaii

ABSTRACT Pulmonary surfactant is a lipid-protein complex that forms a thin film at the air-water surface of the lungs. This surfactant film defines the elastic recoil and respiratory mechanics of the lungs. One generally accepted rationale of using oxygenated perfluorocarbon (PFC) as a respiratory medium in liquid ventilation is to take advantage of its low surface tensions (14–18 mN/m), which was believed to make PFC an ideal replacement of the exogenous surfactant. Compared with the extensive studies of the phospholipid phase behavior of the pulmonary surfactant film at the air-water surface, its phase behavior at the PFC-water interface is essentially unknown. Here, we reported the first detailed biophysical study of phospholipid phase transitions in two animal-derived natural pulmonary surfactant films, Infasurf and Survanta, at the PFC-water interface using constrained drop surfactometry. Constrained drop surfactometry allows in situ Langmuir-Blodgett transfer from the PFC-water interface, thus permitting direct visualization of lipid polymorphism in pulmonary surfactant films using atomic force microscopy. Our data suggested that regardless of its low surface tension, the PFC cannot be used as a replacement of pulmonary surfactant in liquid ventilation where the air-water surface of the lungs is replaced with the PFC-water interface that features an intrinsically high interfacial tension. The pulmonary surfactant film at the PFC-water interface undergoes continuous phase transitions at surface pressures less than the equilibrium spreading pressure of 50 mN/m and a monolayer-to-multilayer transition above this critical pressure. These results provided not only novel biophysical insight into the phase behavior of natural pulmonary surfactant at the oil-water interface but also translational implications into the further development of liquid ventilation and liquid breathing techniques.

SIGNIFICANCE Current liquid ventilation and liquid breathing techniques routinely use perfluorocarbon as the respiratory medium, taking advantage of its high oxygen and carbon dioxide solubility and low surface tensions. However, when the lungs are fully or partially filled with the perfluorocarbon, it is the perfluorocarbon-water interfacial tension rather than the perfluorocarbon-air surface tension that determines the interfacial properties of the alveolar surface. Hence, exogenous surfactant has been found to significantly improve the pathological outcome of liquid ventilation. Here, we report the first detailed biophysical study of lipid polymorphism in natural pulmonary surfactant films at the perfluorocarbon-water interface using constrained drop surfactometry, thus providing novel translational implications into the further development of liquid ventilation and liquid breathing techniques.

INTRODUCTION

Pulmonary surfactant is a lipid-protein complex synthesized by alveolar type II epithelial cells and secreted into the alveolar hypophase coating the inner surface of alveoli (1). Once secreted, the pulmonary surfactant forms a thin film at the air-water surface of the alveolar hypophase by adsorption. The biophysical properties of this pulmonary surfactant film define the elastic recoil and respiratory mechanics of the lungs (2). There are numerous studies about the lipid polymorphism and phospholipid phase behaviors of natural pulmonary surfactant and synthetic phospholipid monolayers spread (3–8) or adsorbed (9) at the air-water surface. A general consensus is that at supraphysiological surface tensions, namely surface tensions above the equilibrium adsorption surface tension (γ_{eq}) of phospholipids, i.e., ~25 mN/m, the pulmonary surfactant monolayer at the air-water surface contains coexisting fluid-like liquid-expanded (LE) and solid-like tilted-condensed (TC) phases (10,11). Within the physiologically relevant low surface tension range, i.e.,

Submitted December 23, 2022, and accepted for publication April 7, 2023.
*Correspondence: yzuo@hawaii.edu
Editor: Tommy Nylander.
https://doi.org/10.1016/j.bpj.2023.04.010

between 0 and ~25 mN/m, however, the pulmonary surfactant film at the air-water surface consists of an interfacial monolayer highly enriched in disaturated phospholipids, mainly dipalmitoyl phosphatidylcholine (DPPC) in the TC phase, plus a three-dimensional surface-associated surfactant reservoir (SASR), mostly composed of unsaturated phospholipids, closely and functionally attached to the interfacial monolayer (9,12,13).

Compared with the extensive studies of the phospholipid phase behavior of the pulmonary surfactant film at the air-water surface, phase behavior of the pulmonary surfactant film at the oil-water interface is essentially unknown. Both the air-water surface and oil-water interface are two-dimensional regions between two immiscible fluids. The menisci of the surface/interface, as well as the resultant mechanical stability, are controlled by the surface energetics and phase behavior of the surfactant film self-assembled at the surface/interface (14). In scenarios that the lungs are partially or fully filled with an oil, such as perfluorocarbons (PFCs) used in liquid ventilation or liquid breathing for deep diving, the alveolar stability, elastic recoil, and respiratory mechanics of the lungs would be largely determined by the phase behavior of pulmonary surfactant film self-assembled at the oil-water interface (15). One generally accepted rationale of using oxygenated PFCs as a respiratory medium in liquid ventilation or liquid breathing is to take advantage of their low surface tensions ($<\gamma_{eq}$ of pulmonary surfactant), which was believed to make PFCs an ideal replacement of the exogenous surfactant (16,17). However, our recent study has showed that although perfluorooctane has a surface tension of 14 mN/m, the PFC-water interfacial tension is as high as 59 mN/m, significantly higher than the γ_{eq} of pulmonary surfactant (15). Our study therefore suggested that PFCs cannot be used as a replacement of the exogenous surfactant, and hence it is crucial to understand the biophysical mechanism by which natural pulmonary surfactant reduces the interfacial tension of the PFC-water interface.

Although the phase behavior of natural pulmonary surfactant at the oil-water interface is largely unknown, there have been a few studies about polymorphism of phospholipid monolayers self-assembled at the oil-water interface due to its importance in understanding emulsification in pharmaceutical, food, and cosmetic industries (14,18). To date, studies of biophysical properties and phase behavior of phospholipid monolayers at the oil-water interface mostly relied on the classical Langmuir film balance or droplet interface bilayers. Using the classical Langmuir film balance, Möhwald and co-workers have studied the effect of various hydrocarbons on self-assembled DPPC and dipalmitoyl phosphatidylethanolamine monolayers at the oil-water interface (19,20). These workers found that depending on the headgroup of the studied phospholipids, hydrocarbons with a chain length close to that of the phospholipid can penetrate into condensed lipid domains, thus disrupting the phospholipid phase behavior at the oil-water interface (19,20). One intrinsic design limitation of using the classical Langmuir film balance to study the oil-water interface is that it requires a stack of oil layers atop the water subphase in a Langmuir trough, which introduces a series of experimental complications, including interfacial instability and inaccurate interfacial tension measurements due to difficulties of maintaining a zero contact angle for the Wilhelmy plate (15,21). Alternatively, droplet interface bilayers (DIBs) are artificial lipid bilayers formed at the interface of two water droplets coated with phospholipid monolayers, approaching each other in an oil phase (22,23). DIBs provide a practical platform of synthetic cell membranes for studying lipid-lipid and lipid-protein interactions at the oil-water interface (22,23). However, it is technically difficult to continuously regulate the interfacial tension of the phospholipid monolayer self-assembled at the oil-water interface of DIBs.

Here, we studied the detailed phospholipid phase behavior of two animal-derived natural pulmonary surfactant films self-assembled at the PFC-water interface using a newly developed experimental method called constrained drop surfactometry (CDS). CDS is a new generation of droplet-based surface tensiometry technique developed in our laboratory to study the biophysics of pulmonary surfactant films at the air-water surface (9,24). We have further developed the CDS technique to extend its application to the oil-water interface (15). Most importantly, we have developed a novel in situ Langmuir-Blodgett (LB) transfer technique that allows direct LB transfer from the oil-water interface of the CDS, thus permitting direct visualization of phase transitions in pulmonary surfactant films at the oil-water interface using atomic force microscopy (15). It was found that natural pulmonary surfactant films undergo continuous LE-TC phase transitions at surface pressures less than the equilibrium spreading pressure (π_{eq}) and a monolayer-to-multilayer transition above π_{eq}. Our results provide not only novel biophysical insight into the phase behavior of natural pulmonary surfactant at the oil-water interface but also translational implications into the further development of liquid ventilation and liquid breathing techniques.

MATERIALS AND METHODS

Materials

Infasurf was extracted from bronchoalveolar lavage of newborn calves. It contained most hydrophobic components of the natural pulmonary surfactant, including cholesterol. Survanta was extracted from minced bovine lung tissues, with additional procedures to remove neutral lipids (mainly cholesterol) and to supplement synthetic DPPC, palmitic acid, and tripalmitin (25). Both surfactant preparations were devoid of the hydrophilic surfactant protein A (SP-A) and had reduced contents of the hydrophobic proteins SP-B and SP-C. Detailed chemical compositions of these two clinical surfactant preparations can be found in Fig. 1 *A* and Table S1 (8). Both surfactant preparations were extracted with chloroform-methanol using a modified Bligh-Dyer method. The chloroform-methanol extracts were dried under a nitrogen stream and redissolved in chloroform to a final

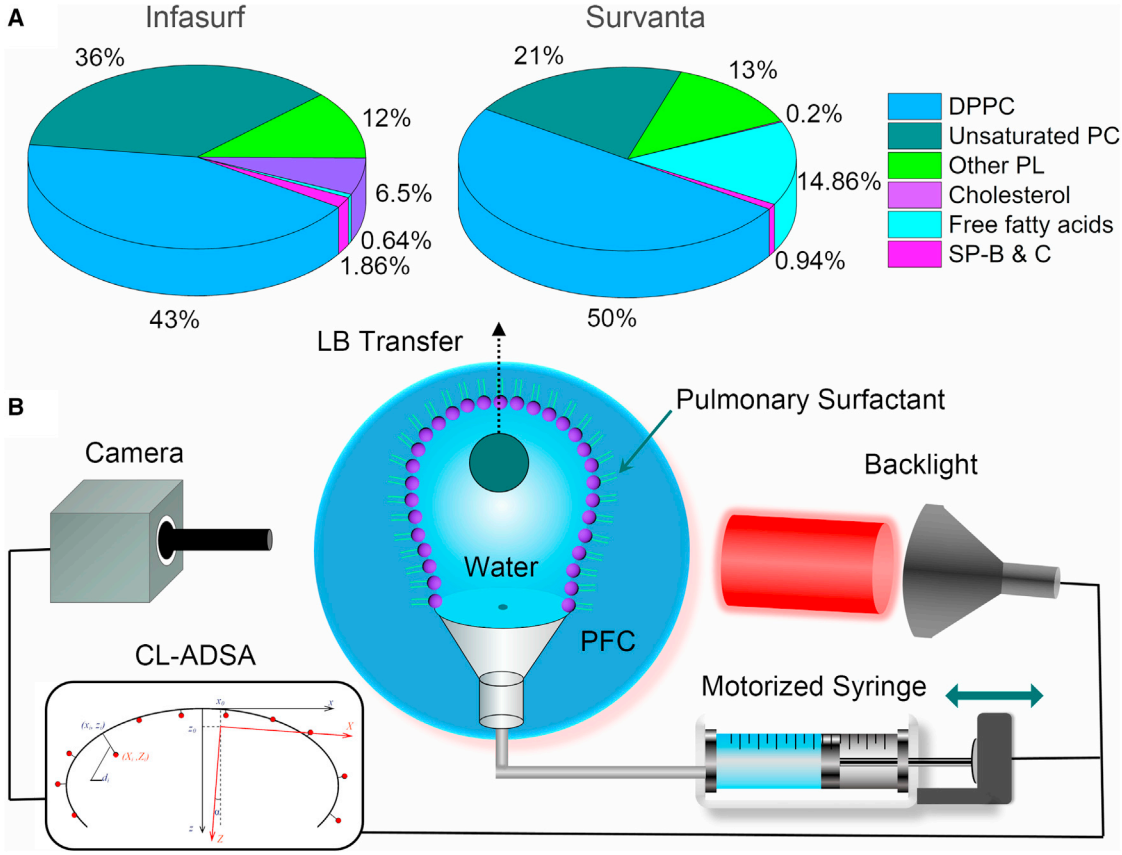

FIGURE 1 (*A*) Lipid and protein compositions (wt %) of two animal-derived pulmonary surfactants, Infasurf and Survanta. DPPC, dipalmitoyl phosphatidylcholine; PL, phospholipid; PC, phosphatidylcholine; SP, surfactant protein. (*B*) Schematic of constrained drop surfactometry for studying pulmonary surfactant film at the perfluorocarbon (PFC)-water interface using a water-in-oil configuration. Since water is lighter than PFC, the water droplet appears as a pendant bubble. Interfacial tension of pulmonary surfactant film-covered droplet is determined in real time photographically from the shape of the droplet using closed-loop axisymmetric drop shape analysis. The pulmonary surfactant film can be Langmuir-Blodgett transferred from the PFC-water interface to a solid substrate under controlled interfacial pressure. To see this figure in color, go online.

concentration of 1 mg/mL. All stock solutions were stored at −20°C until use. Perfluorooctane (C_8F_{18}) was purchased from Sigma-Aldrich (St. Louis, MO, USA) and used without further purification. Water used was Mill-Q ultrapure water (Millipore, Billerica, MA, USA).

CDS

CDS is a new generation of droplet-based surface tensiometry technique developed in our laboratory for studying pulmonary surfactant films at the air-water surface (9,24). CDS uses a 3-mm droplet pedestal with a knife-sharp edge to maintain the droplet integrity even at low surface tensions. The droplet pedestal provides a leakage-proof environment so that the surfactant film is "constrained" at the air-water surface of the droplet without leaking over the pedestal. The pulmonary surfactant film can be compressed and expanded by regulating fluid flow with a motorized syringe. Closed-loop axisymmetric drop shape analysis was used to determine the surface tension and surface area of the droplet in real time (26).

Recently, we have further developed the CDS technique to allow the study of compression isotherms of surfactant film self-assembled at the oil-water interface (15). The oil-water interface can be constructed with either an oil-in-water configuration or a water-in-oil configuration. The resultant droplet shape depends on the relative densities of the oil and water (27). Since perfluorooctane is heavier than water, the water-in-oil configuration assumes the shape of a pendant bubble, while the oil-in-water configuration assumes the shape of a sessile drop.

Specially, a trace amount of surfactant sample (Infasurf or Survanta) was spread at the oil-water interface using a 10-μL microsyringe. The spread film was left undisturbed for 1 min to allow equilibrium and evaporation of the solvent. The evaporated solvent, i.e., chloroform, was expected to be absorbed by the bulk oil phase, i.e., perfluorooctane. Given the tiny amount of spreading (<1 μL), it is unlikely for the evaporated solvent to significantly affect the bulk oil phase. The film-covered water droplet was then slowly expanded to decrease the interfacial pressure to around 5 mN/m. Subsequently, the surfactant film was compressed quasi-statically at a rate of 0.075 cm^2/min, namely 0.3% initial surface area per second. During compression, the interfacial pressure-surface area (π-A) isotherms were recorded. The interfacial pressure (π) was determined from the interfacial tension (γ) using $\pi = \gamma_0 - \gamma$, with $\gamma_0 = 59$ mN/m being the interfacial tension of a clean, surfactant-free PFC-water interface (Fig. S1) (15). All measurements were performed at room temperature (20°C ± 1°C).

LB transfer from the oil-water interface

LB transfer from the oil-water interface was conducted by following a protocol developed elsewhere (15). Briefly, a water-in-oil configuration (Fig. 1 *B*) was used to avoid contamination of the mica substrate submerged in the droplet prior to the LB transfer. The surfactant monolayer was deposited onto the mica surface held by an anticapillary tweezer, by elevating the mica vertically through the oil-water interface at a rate of 1 mm/min, under

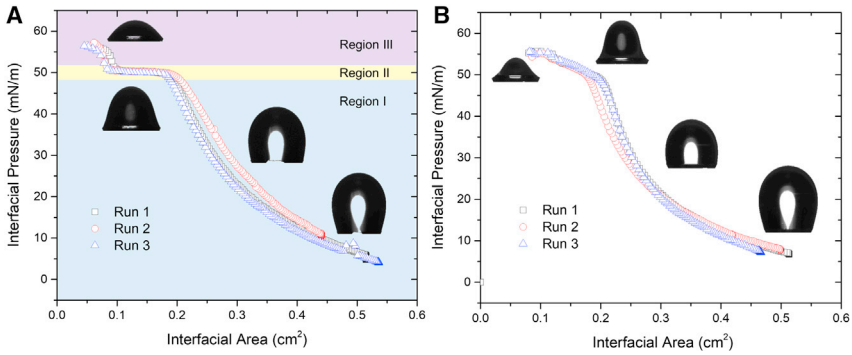

FIGURE 2 Compression isotherms of (*A*) Infasurf and (*B*) Survanta films at the PFC-water interface obtained with the constrained drop surfactometry at room temperature. Insets demonstrate the correlations between the interfacial pressure and the shape of the droplet. All compression isotherms were repeated three times to demonstrate reproducibility. Compression isotherms of the Infasurf film can be divided into three regions: region I: monolayer; region II: monolayer-to-multilayer transition; and region III: multilayer. To see this figure in color, go online.

a constant interfacial pressure (±1 mN/m) controlled by closed-loop axisymmetric drop shape analysis. The deposition ratio of the surfactant film was found to be between 1.1 and 1.4 (15).

Atomic force microscopy

Topographical images of the LB-transferred surfactant film were obtained using an Innova AFM (Bruker, Santa Barbara, CA, USA). Samples were scanned using tapping mode in air by a silicon cantilever with a resonance frequency of 300 kHz and a spring constant of 42 N/m. Images were taken at multiple locations to ensure representativeness and reproducibility. Lateral structures of the samples were analyzed and three-dimensional renderings were produced using Nanoscope Analysis software.

Statistical analysis

Results for phospholipid domain analysis were shown as mean ± standard deviation. $n > 30$ for domains in the Infasurf monolayer, and $n > 70$ for domains in the Survanta monolayer. One-way ANOVA with Tukey's means comparison test was used to determine group differences (OriginPro, Northampton, MA, USA). A value $p < 0.05$ was considered to be statistically significant.

RESULTS

Compression isotherms of Infasurf and Survanta at the PFC-water interface

Fig. 2 shows the typical compression isotherms of Infasurf and Survanta films at the PFC-water interface. Each compression isotherm was repeated at least three times to ensure reproducibility. Insets in Fig. 2 show images of the water-in-oil droplet configuration (i.e., pendant bubble) at various interfacial pressures (π), which demonstrates the correlation between π and the drop shape.

The compression isotherm of the Infasurf film at the PFC-water interface features a fairly flat plateau region at π ~50 mN/m (Fig. 2 *A*). This plateau separates the compression isotherms into three distinct regions. At π lower than this plateau (region I), the Infasurf film is expected to be in a monolayer conformation with a relatively high compressibility. During this plateau (region II), the Infasurf monolayer is transformed into a multilayered conformation by squeezing out fluid phospholipid components. At π higher than this plateau (region III), the Infasurf film assumes a monolayer highly enriched in disaturated phospholipids, indicated by a very low compressibility (i.e., less area reduction required to increase π), with surface-associated multilayers composed of the squeezed-out fluid phospholipids. At π ~56 mN/m (corresponding to a γ ~3 mN/m), the Infasurf film irreversibly collapses, thus reaching the maximum collapse pressure.

The Survanta film at the PFC-water interface shows a compression isotherm similar to that of the Infasurf film, except the monolayer-to-multilayer transition plateau is not as flat as that of Infasurf. Rather, Survanta shows a rising plateau, starting from ~50 mN/m and ending at ~55 mN/m, at which the Survanta film irreversibly collapses (Fig. 2 *B*).

Phase evolution of the Infasurf film at PFC-water interface upon lateral compression

Fig. 3 shows atomic force microscopy (AFM) images of the Infasurf film at the PFC-water interface obtained at increasing π of 30, 40, 50, and 53 mN/m. Reproducibility of these AFM images can be found in Figs. S2–S5. At π of 30, 40, and 50 mN/m, the Infasurf film assumes a monolayer conformation with phase separation, featuring microscale TC domains approximately 1 nm higher than the surrounding LE phase. As shown in Fig. 5 *A*, the average size of these microdomains in the Infasurf monolayer first increases from 2 to 2.8 μm with π increasing from 30 to 40 mN/m and then decreases from 2.8 to 1 μm with π further increasing from 40 to 50 mN/m.

Two additional structural features in the monolayer conformation are worth mentioning. First, the Infasurf monolayer at 40 and 50 mN/m shows isolated protrusions ~4 nm in height, corresponding to the thickness of a fully hydrated phospholipid bilayer (28). At 40 mN/m, these protrusions are preferably concentrated at the TC-LE domain boundaries, thus indicating that they are likely to be individual phospholipid bilayers squeezed out from the interfacial monolayer. Second, in addition to microscale TC domains, the Infasurf monolayer also shows nanoscale TC domains (110 ± 20 nm), which demonstrate a significant abundance

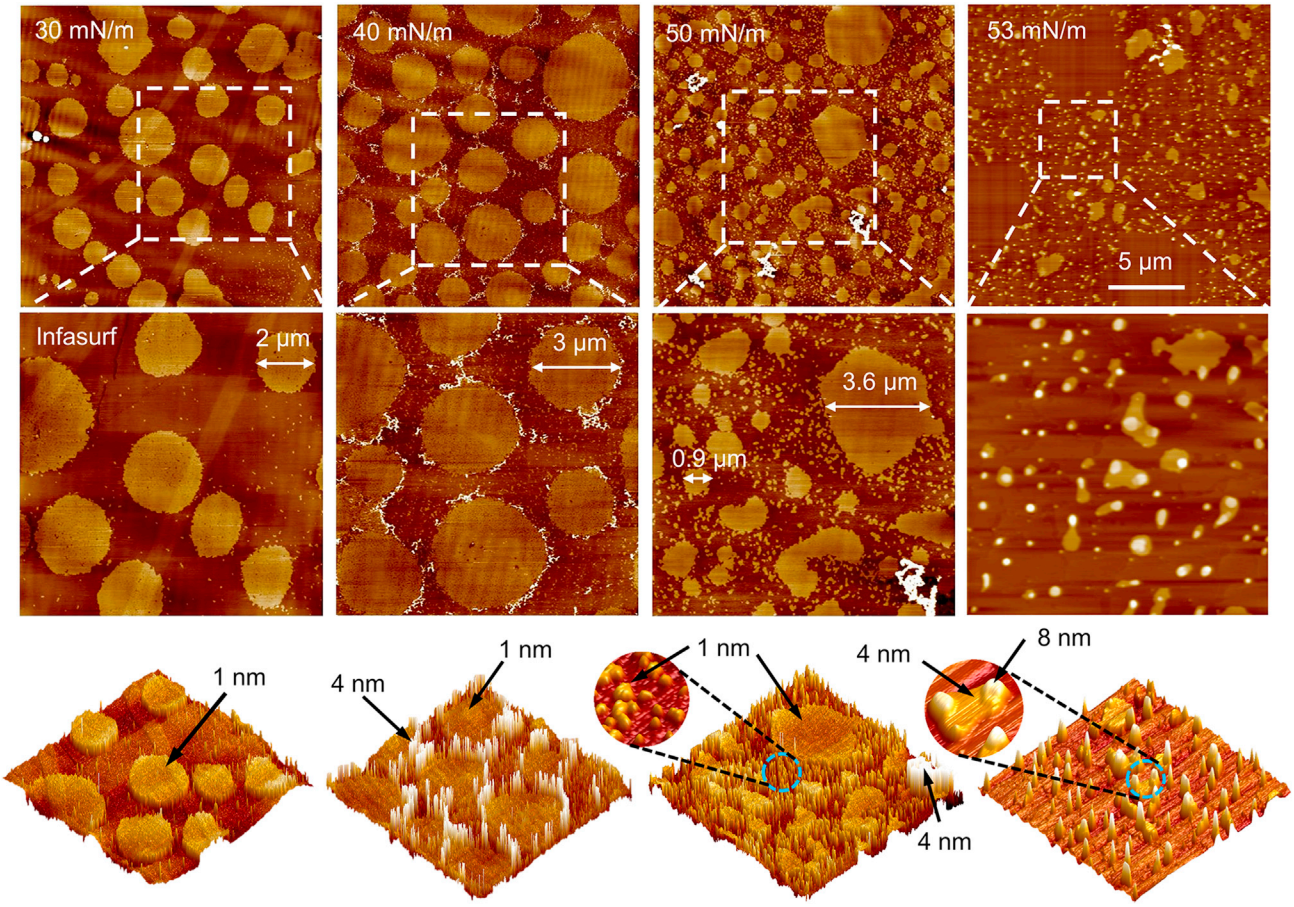

FIGURE 3 Lateral structure and topography of the Infasurf film at the PFC-water interface at four characteristic interfacial pressures, i.e., 30, 40, 50, and 53 mN/m. All AFM images in the top row have the same scanning area of 20 × 20 μm. The z range is 5 nm for all monolayers and 20 nm for multilayers. AFM images in the middle row show zoomed-in images indicated by the white boxes. AFM images in the bottom row show the three-dimensional rendering of the zoomed-in images. Double-headed white arrows indicate the lateral size of domains, and single-headed black arrows indicate the height of structures. Inset of the AFM image at 50 mN/m shows the nanodomains. Inset of the AFM image at 53 mN/m shows the multilayered protrusions. To see this figure in color, go online.

at 50 mN/m. These nanodomains are likely dissociated from the microdomains so that the total surface area covered by the TC domains does not change significantly between 40 and 50 mN/m, although the average size of microdomains at 50 mN/m is much smaller than that at 40 mN/m (Fig. 5 *A*).

At 53 mN/m, i.e., when the Infasurf monolayer is compressed beyond the plateau region, the Infasurf film shows a lateral structure completely different from that at lower π. The Infasurf film assumes a multiplayer conformation with numerous protrusions ranging from 4 to 8 nm in height, corresponding to one or two stacks of phospholipid bilayers.

Phase evolution of the Survanta film at PFC-water interface upon lateral compression

Fig. 4 shows the AFM images of the Survanta film at the PFC-water interface obtained at increasing π of 10, 20, 30, 40, and 55 mN/m. Reproducibility of these AFM images can be found in Figs. S6–S10. Similar to the Infasurf film, the Survanta film assumes a monolayer conformation at π lower than the plateau region shown in Fig. 2 *B*. When π is increased from 10 to 20 mN/m, the average domain size increases from ~3.1 to ~4.7 μm, while the total domain coverage increases from 27% to 50% (Fig. 5 *B*). When π is further increased from 20 to 30 mN/m, the domain size reduces to ~2.8 μm, but the domain coverage increases from 50% to 78% due to an increasing number of domains. At 40 mN/m, most TC domains merge into a somewhat continuous phase. Hence, it is not meaningful to quantify the domain size at this π, while the total domain coverage increases to 89% (Fig. 5 *B*). At 55 mN/m, i.e., when the Survanta monolayer is compressed beyond the plateau region, a number of multilayer protrusions ranging from 4 to 12 nm appear in the Survanta film.

DISCUSSION

Pulmonary surfactant is indispensable for liquid ventilation

Current liquid breathing and liquid ventilation techniques routinely use PFCs as the respiratory medium, mostly

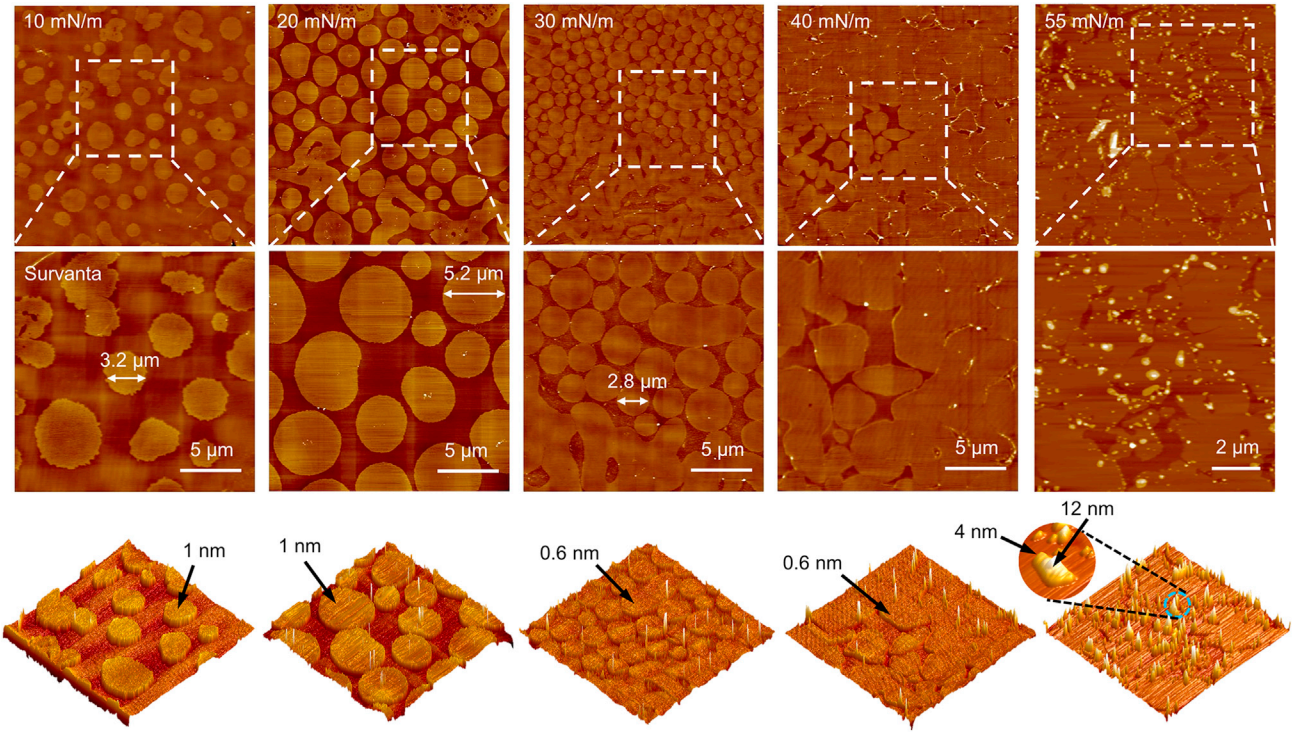

FIGURE 4 Lateral structure and topography of the Survanta film at the PFC-water interface at five characteristic interfacial pressures, i.e., 10, 20, 30, 40, and 55 mN/m. AFM images in the top row have the same scanning area of 50 × 50 μm, except that the scanning area at 55 mN/m is 20 × 20 μm. The z range is 5 nm for all monolayers and 20 nm for multilayers. AFM images in the middle row show zoomed-in images indicated by the white boxes. AFM images in the bottom row show the three-dimensional rendering of the zoomed-in images. Double-headed white arrows indicate the lateral size of domains, and single-headed black arrows indicate the height of structures. Inset of the AFM image at 55 mN/m shows the multilayered protrusions. To see this figure in color, go online.

because of two ideal physicochemical properties of the PFCs. First, PFCs have a high oxygen (~50 mL O_2/dL) and carbon dioxide (140–210 mL CO_2/dL) solubility (16,17). Second, PFCs have very low surface tensions, i.e., 14–18 mN/m, lower than the γ_{eq} of natural pulmonary surfactants (16,17). Hence, it is generally believed that the PFC liquid is an ideal replacement of pulmonary surfactants (16,17). However, when the lungs are fully or partially filled with the PFC liquid, it is the PFC-water interfacial tension rather than the PFC-air surface tension that determines the interfacial properties of the alveolar surface. Our previous (15) and current studies showed that the PFC-water interfacial tensions are significantly higher than the surface tensions of PFCs (e.g., 59 vs. 14 mN/m), thus suggesting that PFCs cannot be used as a replacement of pulmonary surfactants, which are therefore indispensable for liquid breathing and liquid ventilation.

Our in vitro biophysical findings are supported by ex vivo and in vivo data obtained with PFC-filled lungs. Bachofen et al. (29) studied the correlations between the alveolar microstructure and the ex vivo interfacial tensions of PFC-filled excised rabbit lungs. These workers found that the alveolar surface areas of the PFC-filled lungs were significantly smaller than those of the normal air-filled lungs, indicating that a substantially high interfacial tension, rather than the very low surface tension of the PFC (~15 mN/m),

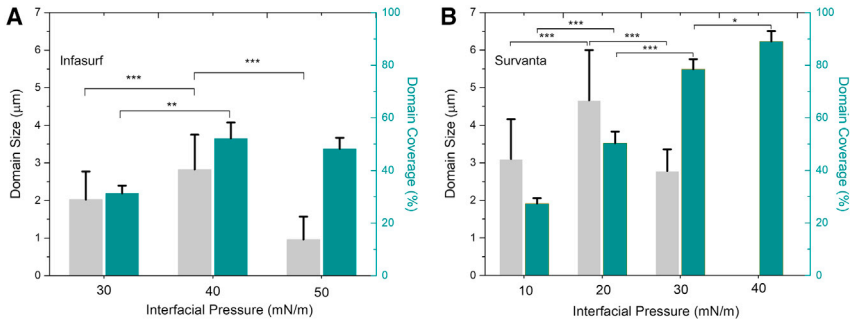

FIGURE 5 Lateral diameter (μm) of the microdomains and the surface area coverage (%) of combined microdomains and nanodomains in the (*A*) Infasurf and (*B*) Survanta monolayers. *p < 0.05, **p < 0.01, ***p < 0.001. To see this figure in color, go online.

defined the alveolar microstructures of the PFC-filled lungs (29). They have further demonstrated the high alveolar interface tension of the PFC-filled lungs by comparing their pressure-volume curves with those of the saline-filled lungs in which the surface tension effects were fully abolished. It was found that the pressure-volume curves of the PFC-filled lungs did not shift to the lower transpulmonary pressure region as the pressure-volume curves of the saline-filled lungs did (29). These ex vivo measurements provided direct physiological implications that despite its low surface tensions, PFC alone cannot be used as a replacement of natural pulmonary surfactant to decrease the alveolar interfacial tension of PFC-filled lungs.

Tarczy-Hornoch et al. (30,31) have directly estimated the interfacial tension of PFC-filled lungs of excised preterm lambs. It was found that the maximum interfacial tension of the PFC-filled lungs at the 20 mL/kg lung volume was 40 mN/m, which was only slightly lower than the maximum surface tension of air-inflated lungs at the same lung volume, i.e., 51 mN/m. However, the maximum alveolar interfacial tension of the preterm lamb lungs was reduced to 27 mN/m when being treated with both liquid ventilation and Survanta (30). The combination of liquid ventilation and exogenous surfactant was also found to improve lung compliance and to reduce the transpulmonary pressure of the preterm lamb lungs (30,31). In addition, other preclinical animal experiments further demonstrated that the exogenous surfactant given before liquid ventilation produced more improvement in the pathological outcomes than no surfactant or surfactant given after liquid ventilation (32,33). Therefore, all available physiological and preclinical data support the need to better understand the biophysical behavior of natural pulmonary surfactant at the PFC-water interface.

Phospholipid phase behavior of pulmonary surfactant films at the PFC-water interface

Compared with the phospholipid phase behavior of pulmonary surfactant films at the air-water surface (3–8), phase transitions of natural pulmonary surfactant films at the PFC-water interface have been largely unknown. Rüdiger et al. (34) found that PFC-assisted liquid ventilation did not alter the intra- and extracellular surfactant content or subtype composition in the bronchoalveolar lavage. These data suggested that PFC does not interfere with surfactant metabolism and homeostasis, likely due to the intrinsic chemical inert properties of the PFC liquids (35,36). Hence, surface energetics and phase transitions of pulmonary surfactant films self-assembled at the PFC-water interface can be considered to be fully driven by biophysical mechanisms. By studying the phase behavior of two animal-derived natural pulmonary surfactant films, Infasurf and Survanta, using the novel CDS technique, we have found several similarities and differences between the phospholipid polymorphism at the air-water surface and at the PFC-water interface.

First, the pulmonary surfactant films assume a monolayer conformation with LE and TC phase separations at π lower than a critical π of $\sim$50 mN/m, known as the equilibrium spreading pressure (π_{eq}), corresponding to a γ_{eq} of $\sim$9 mN/m at the PFC-water interface. This γ_{eq} is much lower than the γ_{eq} of pulmonary surfactant films at the air-water surface, i.e., $\sim$25 mN/m (1). Within the monolayer region (region I of Fig. 2 *A*), the size of the TC domains first increases and then decreases, upon increasing π, for both Infasurf and Survanta monolayers (Fig. 5). A close look at the domain morphology of the Infasurf monolayer (Fig. 3) indicates that the decrease of the average domain size from $\sim$2.8 μm at 40 mN/m to $\sim$1 μm at 50 mN/m is due to dissociation of microdomains into nanodomains uniformly distributed into the LE phase. Since the nanodomains are formed at the expense of the destabilized microdomains, the total TC domain coverage of the monolayer does not change significantly, regardless of the dramatic decrease in domain size (Fig. 5). Similar LE-TC phase transitions and π-dependent variations in domain sizes have been reported in natural pulmonary surfactant films at the air-water surface (6,8). Such a phenomenon was termed phase remixing (3,37), in which dissociation of the microdomains into nanodomains results in a more homogeneous "two-dimensional alloy" that imparts both stability and flexibility to the pulmonary surfactant monolayer (3,6).

Phase remixing was found in both Infasurf and Survanta monolayers at the PFC-water interface (Fig. 5) but likely with different mechanisms. Phase remixing due to dissociation of microdomains into nanodomains appears to require cholesterol (38,39), which is the major compositional difference between Infasurf and Survanta. While Infasurf contains a physiological level of cholesterol (5–8 wt %), Survanta has nearly no cholesterol (<0.2 wt %) (8,40,41). Consequently, no nanodomains are found in the Survanta monolayer (Fig. 4). Nevertheless, phase remixing also occurs in the Survanta monolayer, with the domain size decreasing from $\sim$4.7 μm at 20 mN/m to $\sim$2.8 μm at 30 mN/m. The equilibrium domain size and shape are determined by the balance between line tension at the domain boundaries and intermolecular electrostatic repulsions (42). Therefore, the phase remixing in Survanta is likely due to a line tension decrease and/or increase in the electrostatic repulsion upon monolayer compression.

Second, the pulmonary surfactant films assume a multilayer conformation at π above π_{eq} (region III of Fig. 2 *A*). Similar to Infasurf film at the air-water surface (8,13), the monolayer and multilayer regions are separated by a monolayer-to-multilayer transition plateau at π_{eq} (region II of Fig. 2 *A*), within which the Infasurf monolayer is gradually purified into an interfacial monolayer highly enriched in disaturated phospholipids, plus a SASR mostly composed of unsaturated phospholipids (9,12,13). One major difference between the Infasurf film at the air-water surface and

at the PFC-water interface is the slope of the monolayer-to-multilayer transition plateau. While the transition plateau at the air-water surface spans a region between 40 and 50 mN/m (8,13), the plateau at the PFC-water interface is nearly flat at a constant π_{eq} of 50 mN/m. This can be explained by a stronger steric and/or hydrophobic restriction for conformational changes of lipid molecules at the oil-water interface than those at the air-water surface (18). Consequently, the SASR of the Infasurf film at the PFC-water interface is mainly composed of 1–2 stacks of bilayers, corresponding to a multilayer height of 4 or 8 nm, smaller than the multilayer protrusions of Infasurf found at the air-water surface (8,13).

The Survanta monolayer is transformed into a multilayer at 55 mN/m (Fig. 4). The multilayer structure of the Survanta film at the PFC-water interface is different from that at the air-water surface. Plenty of experimental evidence showed that the multilayer protrusions of the Survanta film at the air-water surface were originated from the LE phase and formed a multilayered matrix surrounding the circular TC domains at the interfacial monolayer (8,13,43). However, at the PFC-water surface, the multilayer protrusions appear to stack onto the TC phase, while the TC domains in the interfacial monolayer is compressed into a somewhat continuous phase, covering nearly 90% of the entire surface area. Survanta is significantly more viscous than Infasurf due to the lack of cholesterol and the supplementation of synthetic DPPC and palmitic acid (41). Differences in the surface viscosity of these two surfactant preparations can be revealed by their differential lateral structures at 40 mN/m (Figs. 3 vs. 4). While a significant amount of bilayer protrusions was found to be squeezed out of the Infasurf monolayer at this surface pressure, only a limited number of isolated protrusions was found on the Survanta monolayer at the same surface pressure. At high π of 55 mN/m, the surface viscosity of Survanta can be several orders of magnitude higher than that of Infasurf (44). Hence, the multilayer structure of the Survanta film at the PFC-water interface could be the result of a synergetic effect of the high surface viscosity and large steric/hydrophobic confinement for the lipid molecules at the oil-water interface (14,18).

CONCLUSIONS

We reported the first detailed biophysical study of phospholipid phase transitions in two animal-derived natural pulmonary surfactant films, Infasurf and Survanta, at the PFC-water interface using CDS. The CDS allows in situ LB transfer from the PFC-water interface, thus permitting direct visualization of lipid polymorphism in pulmonary surfactant films using AFM. Our data suggested that regardless of its low surface tension, the PFC cannot be used as a replacement of pulmonary surfactant in liquid ventilation where the air-water surface of the lungs is replaced with the PFC-water interface that features an intrinsically high interfacial tension. It was found that natural pulmonary surfactant films at the PFC-water interface undergo continuous LE-TC phase transitions at surface pressures less than the equilibrium spreading pressure (π_{eq}), and a monolayer-to-multilayer transition above π_{eq}. These results provided not only novel biophysical insight into the phase behavior of natural pulmonary surfactant at the oil-water interface but also translational implications into the further development of liquid ventilation and liquid breathing techniques.

SUPPORTING MATERIAL

Supporting material can be found online at https://doi.org/10.1016/j.bpj.2023.04.010.

AUTHOR CONTRIBUTIONS

G.L and X.X. carried out the experiments and data analysis. Y.Y.Z. designed the research and oversaw the experiments and analysis. Y.Y.Z. and G.L. wrote the paper. All authors discussed the results.

ACKNOWLEDGMENTS

We thank Dr. Sindhu Row of ONY Biotech for donation of Infasurf samples. We thank Dr. Charles Neal of the Kapi'olani Medical Center for Women and Children for collections of Survanta samples. This research was supported by the National Science Foundation grant number CBET-2011317 (to Y.Y.Z.).

DECLARATION OF INTERESTS

The authors declare no competing interests.

REFERENCES

1. Zuo, Y. Y., R. A. W. Veldhuizen, …, F. Possmayer. 2008. Current perspectives in pulmonary surfactant — inhibition, enhancement and evaluation. *Biochim. Biophys. Acta.* 1778:1947–1977.
2. Parra, E., and J. Pérez-Gil. 2015. Composition, structure and mechanical properties define performance of pulmonary surfactant membranes and films. *Chem. Phys. Lipids.* 185:153–175.
3. Nag, K., J. Perez-Gil, …, K. M. Keough. 1998. Phase transitions in films of lung surfactant at the air-water interface. *Biophys. J.* 74:2983–2995.
4. Discher, B. M., W. R. Schief, …, S. B. Hall. 1999. Phase separation in monolayers of pulmonary surfactant phospholipids at the air-water interface: composition and structure. *Biophys. J.* 77:2051–2061.
5. Knebel, D., M. Sieber, …, M. Amrein. 2002. Fluorescence light microscopy of pulmonary surfactant at the air-water interface of an air bubble of adjustable size. *Biophys. J.* 83:547–555.
6. Zuo, Y. Y., E. Keating, …, F. Possmayer. 2008. Atomic force microscopy studies of functional and dysfunctional pulmonary surfactant films. I. Micro- and nanostructures of functional pulmonary surfactant films and the effect of SP-A. *Biophys. J.* 94:3549–3564.
7. Zuo, Y. Y., R. Chen, …, A. W. Neumann. 2016. Phase transitions in dipalmitoylphosphatidylcholine monolayers. *Langmuir.* 32:8501–8506.

8. Zhang, H., Q. Fan, …, Y. Y. Zuo. 2011. Comparative study of clinical pulmonary surfactants using atomic force microscopy. *Biochim. Biophys. Acta.* 1808:1832–1842.
9. Xu, L., Y. Yang, and Y. Y. Zuo. 2020. Atomic force microscopy imaging of adsorbed pulmonary surfactant films. *Biophys. J.* 119:756–766.
10. Zasadzinski, J. A., J. Ding, …, A. J. Waring. 2001. The physics and physiology of lung surfactants. *Curr. Opin. Colloid Interface Sci.* 6:506–513.
11. Rugonyi, S., S. C. Biswas, and S. B. Hall. 2008. The biophysical function of pulmonary surfactant. *Respir. Physiol. Neurobiol.* 163:244–255.
12. Keating, E., Y. Y. Zuo, …, R. A. W. Veldhuizen. 2012. A modified squeeze-out mechanism for generating high surface pressures with pulmonary surfactant. *Biochim. Biophys. Acta.* 1818:1225–1234.
13. Zhang, H., Y. E. Wang, …, Y. Y. Zuo. 2011. On the low surface tension of lung surfactant. *Langmuir.* 27:8351–8358.
14. Li, G., and Y. Y. Zuo. 2022. Molecular and colloidal self-assembly at the oil–water interface. *Curr. Opin. Colloid Interface Sci.* 62:101639.
15. Li, G., X. Xu, and Y. Y. Zuo. 2023. Langmuir-Blodgett transfer from the oil-water interface. *J. Colloid Interface Sci.* 630:21–27.
16. Wolfson, M. R., and T. H. Shaffer. 2005. Pulmonary applications of perfluorochemical liquids: ventilation and beyond. *Paediatr. Respir. Rev.* 6:117–127.
17. Kaisers, U., K. P. Kelly, and T. Busch. 2003. Liquid ventilation. *Br. J. Anaesth.* 91:143–151.
18. Pichot, R., R. L. Watson, and I. T. Norton. 2013. Phospholipids at the interface: current trends and challenges. *Int. J. Mol. Sci.* 14:11767–11794.
19. Thoma, M., and H. Möhwald. 1994. Phospholipid monolayers at hydrocarbon/water interfaces. *J. Colloid Interface Sci.* 162:340–349.
20. Thoma, M., and H. Möhwald. 1995. Monolayers of dipalmitoylphosphatidylcholine at the oil-water interface. *Colloids Surf. A Physicochem. Eng. Asp.* 95:193–200.
21. Mottola, M., B. Caruso, and M. A. Perillo. 2019. Langmuir films at the oil/water interface revisited. *Sci. Rep.* 9:2259.
22. Bayley, H., B. Cronin, …, M. Wallace. 2008. Droplet interface bilayers. *Mol. Biosyst.* 4:1191–1208.
23. Stephenson, E. B., J. L. Korner, and K. S. Elvira. 2022. Challenges and opportunities in achieving the full potential of droplet interface bilayers. *Nat. Chem.* 14:862–870.
24. Valle, R. P., T. Wu, and Y. Y. Zuo. 2015. Biophysical influence of airborne carbon nanomaterials on natural pulmonary surfactant. *ACS Nano.* 9:5413–5421.
25. Bernhard, W., J. Mottaghian, …, C. F. Poets. 2000. Commercial versus native surfactants. Surface activity, molecular components, and the effect of calcium. *Am. J. Respir. Crit. Care Med.* 162:1524–1533.
26. Yu, K., J. Yang, and Y. Y. Zuo. 2016. Automated droplet manipulation using closed-loop axisymmetric drop shape analysis. *Langmuir.* 32:4820–4826.
27. Yang, J., K. Yu, and Y. Y. Zuo. 2017. Accuracy of axisymmetric drop shape analysis in determining surface and interfacial tensions. *Langmuir.* 33:8914–8923.
28. Regan, D., J. Williams, …, W. Langbein. 2019. Lipid bilayer thickness measured by quantitative DIC reveals phase transitions and effects of substrate hydrophilicity. *Langmuir.* 35:13805–13814.
29. Bachofen, H., S. Schürch, and F. Possmayer. 1994. Disturbance of alveolar lining layer: effects on alveolar microstructure. *J. Appl. Physiol.* 76:1983–1992.
30. Tarczy-Hornoch, P., J. Hildebrandt, …, J. C. Jackson. 1996. Effects of exogenous surfactant on lung pressure-volume characteristics during liquid ventilation. *J. Appl. Physiol.* 80:1764–1771.
31. Tarczy-Hornoch, P., J. Hildebrandt, …, J. C. Jackson. 1998. Surfactant replacement increases compliance in premature lamb lungs during partial liquid ventilation in situ. *J. Appl. Physiol.* 84:1316–1322.
32. Mrozek, J. D., K. M. Smith, …, M. C. Mammel. 1997. Exogenous surfactant and partial liquid ventilation: physiologic and pathologic effects. *Am. J. Respir. Crit. Care Med.* 156:1058–1065.
33. Nishina, K., K. Mikawa, …, H. Obara. 2005. The efficacy of fluorocarbon, surfactant, and their combination for improving acute lung injury induced by intratracheal acidified infant formula. *Anesth. Analg.* 100:964–971.
34. Rüdiger, M., S. Wendt, …, M. Ochs. 2007. Alterations of alveolar type II cells and intraalveolar surfactant after bronchoalveolar lavage and perfluorocarbon ventilation. An electron microscopical and stereological study in the rat lung. *Respir. Res.* 8:40.
35. Riess, J. G. 2005. Understanding the fundamentals of perfluorocarbons and perfluorocarbon emulsions relevant to in vivo oxygen delivery. *Artif. Cells Blood Substit. Immobil. Biotechno.* 33:47–63.
36. Krafft, M. P. 2001. Fluorocarbons and fluorinated amphiphiles in drug delivery and biomedical research. *Adv. Drug Deliv. Rev.* 47:209–228.
37. Discher, B. M., K. M. Maloney, …, S. B. Hall. 1996. Lateral phase separation in interfacial films of pulmonary surfactant. *Biophys. J.* 71:2583–2590.
38. Discher, B. M., K. M. Maloney, …, S. B. Hall. 1999. Neutral lipids induce critical behavior in interfacial monolayers of pulmonary surfactant. *Biochemistry.* 38:374–383.
39. Discher, B. M., K. M. Maloney, …, S. B. Hall. 2002. Effect of neutral lipids on coexisting phases in monolayers of pulmonary surfactant. *Biophys. Chem.* 101-102:333–345.
40. Blanco, O., and J. Pérez-Gil. 2007. Biochemical and pharmacological differences between preparations of exogenous natural surfactant used to treat Respiratory Distress Syndrome: role of the different components in an efficient pulmonary surfactant. *Eur. J. Pharmacol.* 568:1–15.
41. Rüdiger, M., A. Tölle, …, B. Rüstow. 2005. Naturally derived commercial surfactants differ in composition of surfactant lipids and in surface viscosity. *Am. J. Physiol.* 288:L379–L383.
42. McConnell, H. M. 1991. Structures and transitions in lipid monolayers at the air-water interface. *Annu. Rev. Phys. Chem.* 42:171–195.
43. Alonso, C., T. Alig, …, J. A. Zasadzinski. 2004. More than a monolayer: relating lung surfactant structure and mechanics to composition. *Biophys. J.* 87:4188–4202.
44. Zasadzinski, J. A., C. Alonso, …, A. J. Waring. 2008. Relationships between surface viscosity, monolayer phase behavior, and the stability of lung surfactant monolayers. *In* Structure and Dynamics of Membranous Interfaces, pp. 341–383.